A normal-pressure MWPC for beam diagnostics at RIBLL2*

TANG Shu-Wen(唐述文)[1,2;1)] MA Peng(马朋)[1] DUAN Li-Min(段利敏)[1]
SUN Zhi-Yu(孙志宇)[1] LU Chen-Gui(鲁辰桂)[1] YANG He-Run(杨贺润)[1]
HU Rong-Jiang(胡荣江)[1] HUANG Wen-Xue(黄文学)[1] XU Hu-Shan(徐瑚珊)[1]

[1] Institute of Modern Physics, Chinese Academy of Sciences, Lanzhou 730000, China
[2] University of Chinese Academy of Sciences, Beijing 100049, China

Abstract: A normal pressure MWPC for beam diagnostics at RIBLL2 has been developed, which has a sensitive area of 80 mm×80 mm and consists of three-layer wire planes. The anode plane is designed with a wider frame to reduce the discharge and without using protection wires. The detector has been tested with a ^{55}Fe X-ray source and a 200 MeV/u ^{12}C beam from CSRm. A position resolution better than 250 μm along the anode wires and a detection efficiency higher than 90% have been achieved.

Key words: MWPC, beam diagnostics, delay line readout, position resolution, detection efficiency

PACS: 29.40.Cs, 29.40.Gx **DOI:** 10.1088/1674-1137/37/6/066002

1 Introduction

The production of the radioactive ion beam (RIB), which started in the middle of the 1980s [1], opened a new domain in nuclear physics and astrophysics. Tens of radioactive ion beam lines have been built worldwide. Two of them, the First Radioactive Ion Beam Line in Lanzhou (RIBLL1) [2] and the Second Radioactive Ion Beam Line in Lanzhou (RIBLL2) [3], were constructed at the Heavy Ion Research Facility in Lanzhou (HIRFL) [4], which is located at the Institute of Modern Physics (IMP), the Chinese Academy of Sciences. RIBLL2 is a double achromatic anti-asymmetry spectrometer to produce the RIBs with a primary ion beam up to 1 GeV/u for either external target experiment or storage ring mass spectroscopy. Normally, the type of diagnostic detector used for tens of MeV/u RIBs is selected to be a Parallel Plate Avalanche Counter (PPAC) [5] or a low-pressure Multi-Wire Proportional Chamber (MWPC) [6]. As for RIBs with energy of hundreds of MeV/u or higher, these detectors will suffer from low detection efficiency. In order to increase the detection efficiency, a normal pressure MWPC is constructed for beam diagnosis at RIBLL2. In the case of high vacuum of 10^{-9} mbar at RIBLL2, a special designed vacuum chamber to contain the MWPC is constructed as well.

In this paper, the design of the MWPC and its readout will be described, and the performance tested with 5.9 keV X-rays from a ^{55}Fe source and a 200 MeV/u ^{12}C beam from CSRm will be also presented.

2 Design and construction

2.1 Detector container

Figure 1 shows the schematic layout of RIBLL2. It consists of 4 dipoles and 20 quadruple magnets, and its

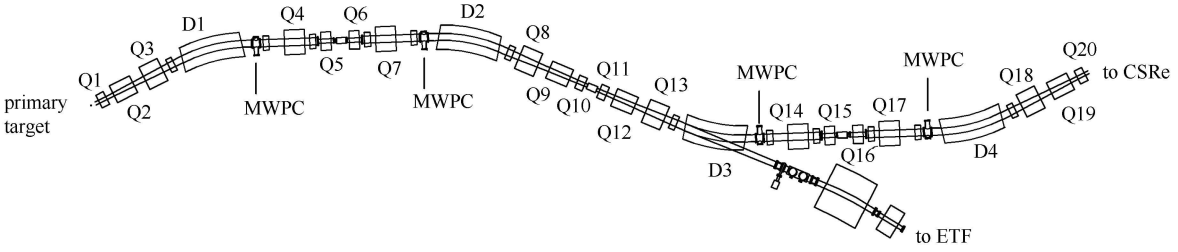

Fig. 1. Schematic layout of RIBLL2 and mounting positions of the MWPCs.

Received 11 July 2012
∗ Supported by National Natural Science Foundation of China (11079044)
1) E-mail: tangsw@impcas.ac.cn

total length is about 55 m. The primary beam extracted from CSRm [7] bombards a target located at the entrance of RIBLL2 to produce the radioactive ion beams through the projectile fragmentation. The RIBs are purified and transported either to the external target facility (ETF) or to CSRe for experiments [8]. In order to monitor the beam profile when tuning the RIBLL2, MWPCs are employed. The positions where the MWPCs are mounted are indicated in the figure.

In order to operate a normal-pressure MWPC in such an ultra high vacuum of 10^{-9} mbar, each MWPC is mounted inside a movable stainless steel pocket which is controlled by a step motor. Fig. 2 shows a schematic drawing of the pocket. In order to sustain one atmospheric pressure difference and to affect the beam as slightly as possible, 0.1 mm stainless steel foils are chosen for the pocket windows. With such a device, the MWPC can be moved in and out of the beam pipe freely.

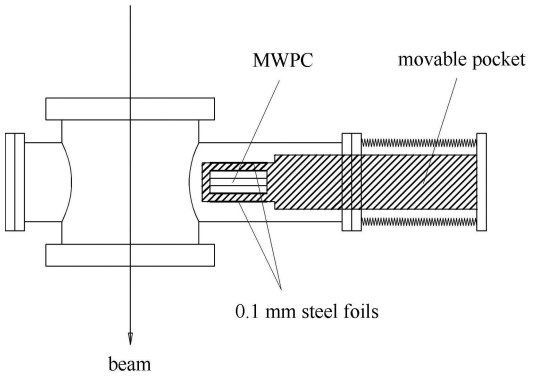

Fig. 2. The special design to insert the normal-pressure MWPC into the beam line with an ultra high vacuum.

2.2 Detector description

Figure 3 shows the layout of the MWPC wire planes. The anode plane is sandwiched between two cathode planes, and the distance between the anode and each cathode is 3 mm. All of the electrode frames are made from printed circuit board (PCB). The active area of the whole MWPC is 80 mm×80 mm. The anode plane consists of 20 Au-W parallel arranged wires of 25 μm in diameter with 4 mm spacing. In order to avoid the dramatically increasing electric field and reduce the spark at the boundaries of the chamber, the traditional way is to substitute the end wires with protection wires in larger diameters. However, this could shrink the sensitive area of the detector. During the research, we found the gain at the boundaries would not increase if the end wires were away from the frame. Therefore, the inner length of the frames is designed as 84 mm×84 mm, and the distance between the end wires and the inner edge of the frame is 2 mm. All the anode wires are soldered together and only one fast time signal output is provided to trigger the data acquisition (DAQ) system. Each of the cathode planes consists of 80 Be-Cu parallel arranged wires of 75 μm in diameter with 1 mm spacing. Every two adjacent cathode wires are soldered together to form one readout strip of 2 mm in width. Both cathodes are placed orthogonally to each other. All the wires are positioned and tensed with a programmable winding machine. The accuracy of the positioning of the wires is about 25 μm, and the tension provided on all wires is 70 g.

For extracting the signals from the cathodes, the delay line technique is employed. The commercial DIP delay line module 1520 from Data Delay Devices company [9] is selected. Each module has 10 taps fixed onto it, and 4 modules are used for one cathode plane in our case.

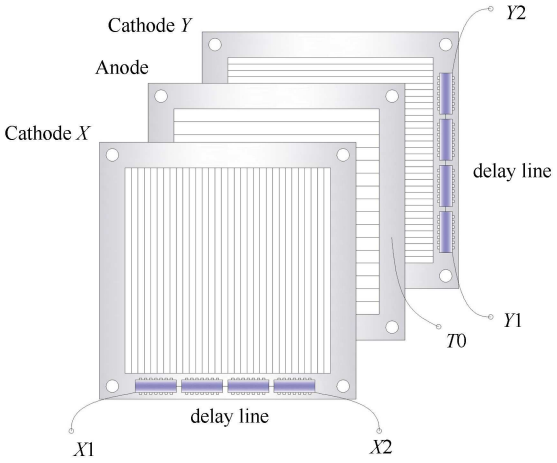

Fig. 3. Structure of the MWPC used for beam diagnostics.

From the viewpoint of spatial resolution, it is better to choose a delay line with longer delay time, but this will decrease the efficiency. We chose 40 ns delay line modules to balance the spatial resolution and the efficiency. Table 1 lists the characteristics of the module. The nominal delay time between two adjacent readout wires is 4 ns, which corresponds to a 2 mm distance, and the nominal tolerance is 0.2 ns. The intrinsic position uncertainty caused by the delay line is estimated to be 50 μm.

Table 1. Characteristics of the delay line module.

parameter	value
number of taps	10
total delay	(40±2) ns
delay between taps	(4±0.2) ns
characteristic impedance	50 Ω
3dB bandwidth	43.75 MHz
rising time	8 ns

With the delay line readout technique, only two output signals are needed for each cathode (see also Fig. 3). The position can be calculated with the following equations:

$$x=k_x(T_{x1}-T_{x2}), \quad (1)$$

$$y=k_y(T_{y1}-T_{y2}), \quad (2)$$

where T_{x1} and T_{x2} are the time from both ends of Cathode X, T_{y1} and T_{y2} are the time of Cathode Y, and k_x and k_y are constant values depending on the width of detector and the electronics, respectively.

3 Test results

The performance of the assembled MWPCs has been tested with a radioactive ion source and the beam. The position (spatial) resolutions of the MWPCs were tested with a 5.9 keV X-ray ^{55}Fe source, and their detection efficiencies were tested with the slow extracted ^{12}C beam of 200 MeV/u from CSRm.

3.1 Test with a ^{55}Fe source

During the test, the signals from the anode and two cathodes are first sent into a fast preamplifier FTA810, and then a constant fraction discriminator CF8000. After that, the cathode signals are input into a PXI TDC module [10] based on the HPTDC [11] chips to record the time information. The DAQ system is triggered by the anode signal.

The MWPC was operated at a high voltage of 1950 V under normal pressure with the gas flow mode. The filling gas was a mixture of 80% Ar and 20% CO_2, and the gas flow rate was about 1.8 l/h. During the test, a collimator with 3 slits was used for position calibration. Each slit is 0.18 mm wide and 1.8 mm apart from each other. The ^{55}Fe source and the collimator moved along the anode wires step by step under the control of a step motor with a step length of 5.4 mm and an accuracy of 25 μm.

Figure 4(a) shows the measured position spectrum, in which each peak represents the position of one of the slits. By fitting the positions the performance of the MWPC detector can be evaluated. Fig. 4(b) shows both the obtained integral nonlinearity (INL) and differential nonlinearity (DNL). In the full range of this detector, the INL is within 0.42 mm (0.5%) and the DNL is within 0.33 mm (0.4%). Fig. 4(c) shows the corresponding position resolution distribution. Obviously, the spatial resolution is better than 250 μm in the full detector range, and the average value is measured to be σ=(186±32) μm.

3.2 Test with a 200 MeV/u ^{12}C beam

To obtain the detection efficiencies of the MWPC detectors, three MWPCs were mounted sequentially in one of the beam lines of the CSRm. The distance between each two MWPCs was 15 cm. A ^{12}C beam with an energy of 200 MeV/u was used for the test. The electronics used were similar to those in the X-ray test, except that a downstream plastic scintillator signal was used to trigger the DAQ system.

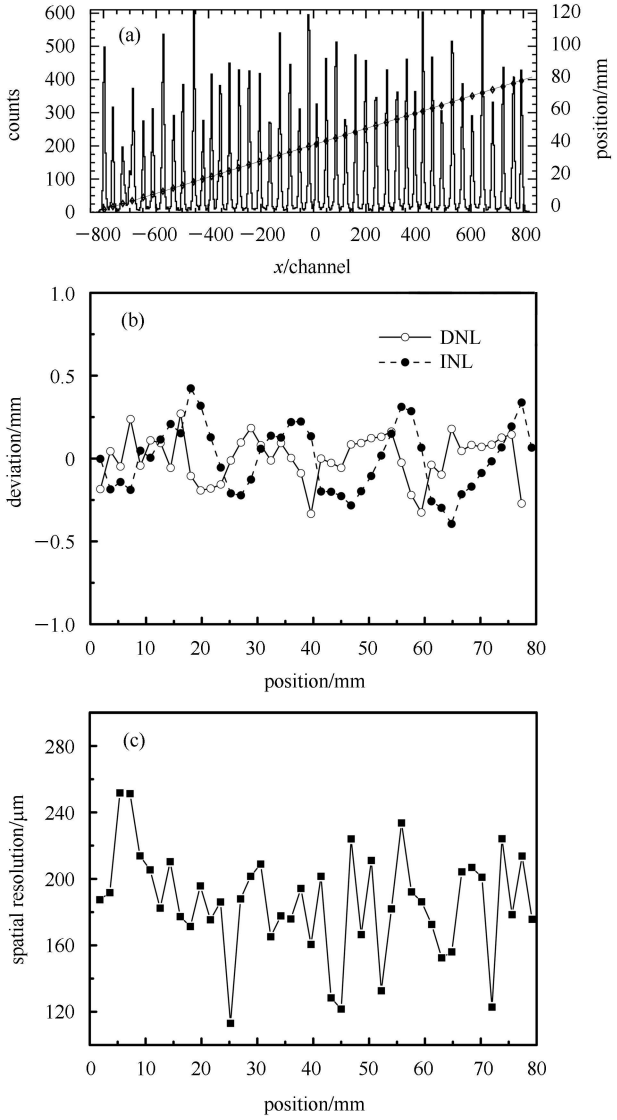

Fig. 4. Position spectrum (a), nonlinearities (b) and spatial resolution (c) measured with a ^{55}Fe source. INL represents the integral nonlinearity, and DNL the differential nonlinearity, respectively.

Figure 5(a) shows a typical ^{12}C beam profile monitored with a MWPC. The lines parallel to the x axis represent the anode wires. The position resolution was determined in the following way. For x direction, we can calculate the position of a charged particle in MWPC$_2$

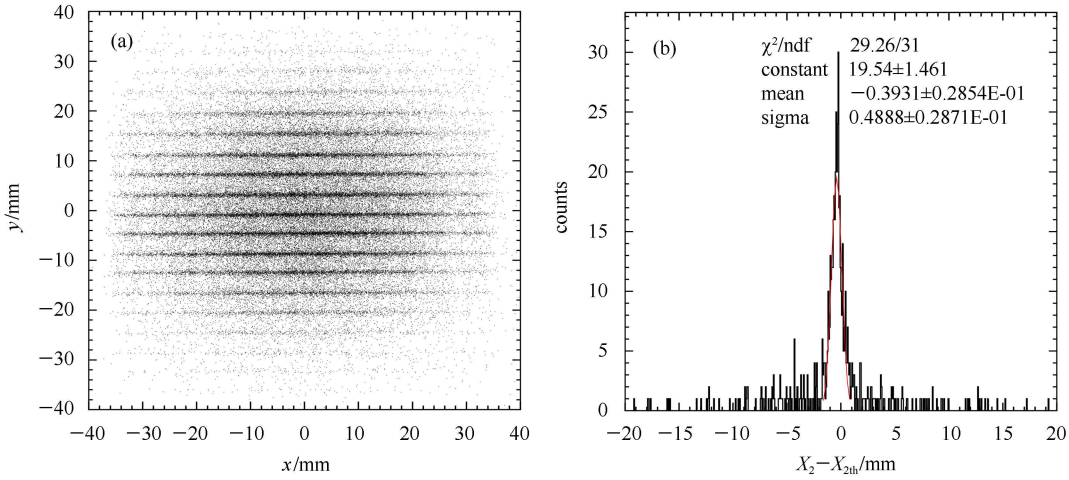

Fig. 5. (a)Beam profile of ^{12}C monitored by the MWPC. (b)Position resolution on X plane.

with the trajectory determined by $MWPC_1$ and $MWPC_3$, which is labeled as $x_{2\mathrm{th}}$, then the difference between $x_{2\mathrm{th}}$ and x_2 is plotted in Fig. 5(b). The resolution is σ_{x0}=(489±29) μm, which is contributed by all the three MWPCs. Therefore, the position resolution for one MWPC is σ_x=(282±17) μm. As for y direction, the position resolution is $\sigma_y=s/\sqrt{12}$=1.15 mm.

The detection efficiency can be calculated by the following equations:

$$\eta_x=\frac{N_{123x}}{N_{13x}}, \tag{3}$$

$$\eta_y=\frac{N_{123y}}{N_{13y}}, \tag{4}$$

where N_{13} is the number of events detected with the 1$^{\mathrm{st}}$ and 3$^{\mathrm{rd}}$ MWPC (to assure the ion has passed all the three MWPCs), N_{123} is the number of events detected by the 2$^{\mathrm{nd}}$ MPWC among all the N_{13} events, and the indices x and y represent x and y directions, respectively.

We applied 1855 V bias for the detectors and tested them with the beam intensity as high as 10^5 pps. The detection efficiency we achieved was 94.9% for x direction and 90.1% for y direction. This performance fully reaches the requirement of the beam diagnostics at RIBLL2.

4 Summary

We have developed a normal-pressure MWPC for beam diagnostics at RIBLL2. The MWPC consists of three-layer wire planes and can work at normal pressure with a special designed container. We have tested the MWPC with a ^{55}Fe X-ray source and achieved a very good position resolution and linearity. The spatial resolution along the anode wires for the whole detector is better than 250 μm. The integral nonlinearity is within 0.5% and the differential nonlinearity is within 0.4%. We have also tested the MWPC with a 200 MeV/u ^{12}C beam at the intensity of 10^5 pps and get the detection efficiency higher than 90%. The tests show that the MWPC can work properly as a beam diagnostic detector for $Z\geqslant 6$ beams with energy $\leqslant$200 MeV/u. In the future, we will test it with lighter and higher-energy beams.

References

1 Tanihata I, Hamagaki H, Hashimoto O et al. Phys. Rev. Lett., 1985, **55**: 2676–2679
2 SUN Z Y, ZHAN W L, GUO Z Y et al. Nucl. Instrum. Methods A, 2003, **503**: 496–503
3 SONG M T, YANG X D, XIA J W et al. High Energy Phys. Nucl. Phys., 2001, **25**: 443–447 (in Chinese)
4 ZHAN W L, XIA J W, ZHAO H W et al. Nucl. Phys. A, 2008, **805**: 533c–540c
5 GENG P, DUAN L M, MA P et al. Nucl. Phys. Rev., 2010, **27**: 450–454
6 LI Z H, CHEN T, YE Y L et al. High Energy Phys. Nucl. Phys., 2002, **26**: 964–970 (in Chinese)
7 XIA J W, ZHAN W L, WEI B W et al. High Energy Phys. Nucl. Phys., 2006, **30**: 335–343 (in Chinese)
8 TU X L, XU H S, WANG M et al. Phys. Rev. Lett., 2011, **106**: 112501
9 http://www.datadelay.com
10 LIU X H, AN Q, LIU S B et al. Nuclear Techniques, 2009, **32**: 632–635
11 Christiansen J, Marchioro A, Morieira P et al. Proc. the 6th Workshop on Electronics for LHC Experiments, Krakow, Poland, 2000